Ecological Indicators 121 (2021) 107105

Contents lists available at ScienceDirect

Ecological Indicators

journal homepage: www.elsevier.com/locate/ecolind

A 15-year spatio-temporal analysis of plant β-diversity using Landsat time series derived Rao's Q index

Siddhartha Khare [a,b,*], Hooman Latifi [c,d], Sergio Rossi [a,e]

[a] Département des Sciences Fondamentales, Université du Québec à Chicoutimi, Canada
[b] Department of Biology, McGill University, Montreal, QC H3A 1B1, Canada
[c] Department of Photogrammetry and Remote Sensing, Faculty of Geodesy and Geomatics Engineering, K. N. Toosi University of Technology, Tehran, Iran
[d] Department of Remote Sensing, University of Würzburg, Germany
[e] Key Laboratory of Vegetation Restoration and Management of Degraded Ecosystems, Guangdong Provincial Key Laboratory of Applied Botany, South China Botanical Garden, Chinese Academy of Sciences, Guangzhou, China

ARTICLE INFO

Keywords:
β-diversity
Rao's Q index
Time series
NDVI
MSAVI
Google Earth Engine

ABSTRACT

Understanding temporal dynamics of plant biodiversity is crucial for conservation strategies at regional and local levels. The mostly applied hitherto methods are based on field observations of the plant communities and the related taxa. Satellite earth observation time series offer continuous and wider coverage for the assessment of plant diversity, especially in remote areas. Theoretical basis and large-scale solutions for assessing beta-diversity have been recently presented. Yet landscape-scale and context-based analysis are missing. We assessed temporal β-diversity using Raós Q diversity derived from Landsat-based vegetation indices by considering the effect of ERA-5 monthly aggregates environmental factors (temperature and precipitation) extracted using Google Earth Engine (GEE), land use classes, and two common vegetation indices. We derived 15-year Rao's Q diversity using Landsat-7 based normalized difference vegetation index (NDVI) and modified soil-adjusted vegetation index (MSAVI). We evaluated the temporal turnover in Rao's Q on multiple land use classes, including agriculture, intact forest and areas affected by and invasive species. Vegetation index and Rao's Q diverged between pre- and post- monsoon seasons. Rao's Q had higher temporal turnover with NDVI than MSAVI for all vegetation classes, however the latter showed higher sensitivity towards temperature and precipitation. Moreover, agriculture generally showed higher variability than forest and invasive species. The temporal turnover was correlated between NDVI and MSAVI for all vegetation classes, which indicated that the variability among vegetation types was directly related to spectral heterogeneity. Furthermore, MSAVI was less sensitive to the effect of soil in assessing the vegetation indices, which resulted in higher global sensitivity of Q_{MSAVI}. Near infrared and red spectra used in vegetation indices are able to capture a small variation in leaf traits reflectance for vegetation types. Here, the β-diversities and their temporal dynamics derived from the vegetation indices differed based on their sensitivity to soil, vegetation density and seasonality. This approach and its open source implementation can be tested for different forest ecosystems at varying spatial scales.

1. Introduction

Despite the accuracy and spatial detail achieved by conventional field-based surveys of sample-based assessments of plant diversity over large areas are still considered as difficult (mono-temporally) or infeasible (multi-temporally) due to the vast time, logistics and manpower required (Gillespie et al., 2008; Hernández-Stefanoni et al., 2012). This is even more prohibitive over remote mountainous areas, where a substantial part of global biodiversity hotspots are located. Remote sensing can efficiently contribute to assess biodiversity through spatially-explicit and continuous imagery. Previous studies provided evidence for general and context-specific feasibility of optical satellite data for biodiversity assessment, in particular from management perspectives (Khare et al., 2018; Kissling et al., 2018; Vihervaara et al., 2017).

Indices and variables derived from optical remote sensing data have shown correlations with field observations on biodiversity, including both spatial and temporal variations (Khare et al., 2019a; Lausch et al., 2016; Rocchini et al., 2019b). From the conventional set of well-known

* Corresponding author.
E-mail address: siddhartha.khare@gmail.com (S. Khare).

https://doi.org/10.1016/j.ecolind.2020.107105
Received 2 June 2020; Received in revised form 9 September 2020; Accepted 19 October 2020
Available online 26 October 2020

measures used for quantifying local and regional diversity, such as α, β and γ diversities, the β –diversity, i.e. the share of spatial variation in species abundance and composition between two sites (Whittaker, 1972) was introduced to measure the relative species abundance, richness and functional gradients (Rocchini, 2007). This concept was further implemented to apply the spectral heterogeneity information extracted from remote sensing data on a multivariate basis for β-diversity assessments, and gained increasing popularity in successive studies (Hernández-Stefanoni et al., 2012; Khare et al., 2019a; Khare et al., 2018, Rocchini et al., 2017; Rocchini et al., 2009a).

Rao's Q index (Rao, 1982) was stated to correct for the arithmetical drawbacks of Shannon and Rényi indices by taking into account the numerical magnitude and pairwise distance of pixel values in the multivariate context in addition to the richness and relative abundance (Rocchini, 2007). Rocchini et al. (2017) further extended the concept of Rao's Q diversity and provided a remote sensing based approach to assess the β-diversity with an example of large-scale analysis on continental MODIS data. Khare et al. (2019a) tested this concept on a multiple spatial resolution and showed its ability to overcome the shortcomings of the Shannon index with an additional multi-scale

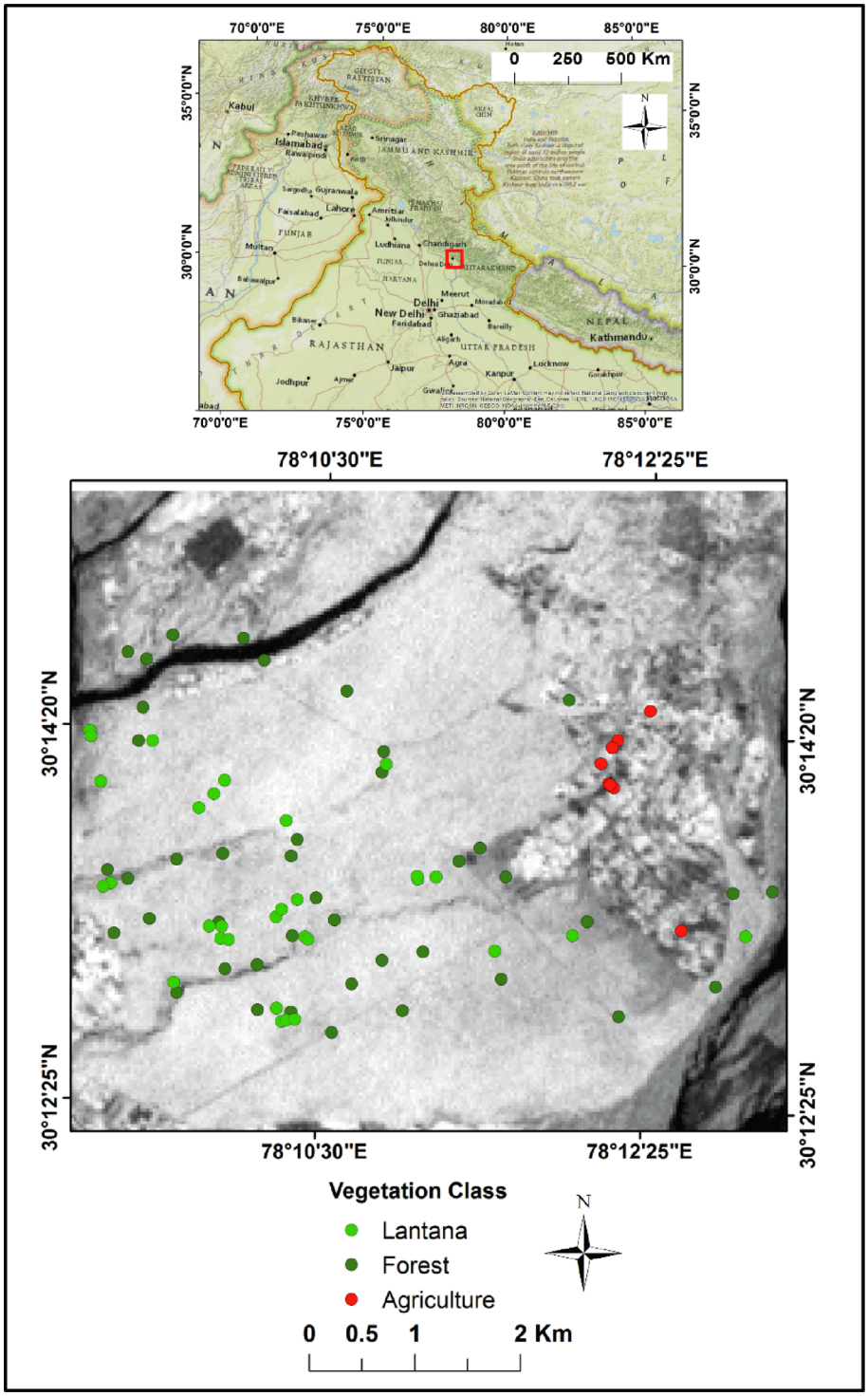

Fig. 1. Study site showing the Thano forest area for NDVI Landsat 7 ETM + and training sample points of three different vegetation classes (N = 100).

analysis, which suggested a notable increase in the estimated diversity in finer spatial resolutions and smaller window size. Within a heterogeneously-structured study site, the β-diversity estimation was most realistic at lower overstory density and visible understory due to the unconstrained spectral signatures provided by optical data. The spectral variation could therefore be related to different land use and seasonal variations and may be considered as an important proxy for species diversity (Palmer et al., 2002; Torresani et al., 2019).

This approach still lacks integration of a temporal dimension, which 1) can be crucial in the context of monitoring β-diversity and 2) complements the currently available multi-scale approach, in particular provided that data at different spatial resolutions are multi-temporally available. A very recent benchmark study by Rocchini et al. (2019b) estimated temporal β-diversity using Rao's Q diversity on multi-temporal MODIS-derived normalized difference vegetation index (NDVI) and showed its potential for plotting the spatiotemporal variability in biodiversity analysis. However, Rocchini et al. (2019b) asked for further implementation on other satellite sensor types, as well as on further 2D matrices including species-plot arrays or indices rather than NDVI.

In this paper, we used Rao's Q to assess changes in biodiversity during 2000–2015 within the moist deciduous forest in the Western Himalayan region, India. We aim to 1) develop an approach for temporal analysis using Landsat-based Rao's Q diversity; 2) assess the performance of Rao's Q under multiple vegetation classes; and 3) to compare multi-temporal Rao's Q diversity derived for NDVI and modified soil-adjusted vegetation index (MSAVI) and their temporal variations. We tested the hypothesis that MSAVI derived spatial Rao's Q provides higher spatial heterogeneity than the index calculated with NDVI due to its lesser sensitivity to soil factors, which plays an important role in reducing the soil effects on different land use types.

2. Materials and methods

2.1. Study area

The study area is located in the Western Himalayan region of Doon valley, Uttarakhand, India (29° 55′ to 30° 30′ N and 77° 35′ to 78° 24′E). This area is considered as part of a global biodiversity hotspot, i.e. a region characterized by both exceptional levels of plant endemism and serious rates of habitat losses. We selected Thano forest as a study area due to its wide variability in canopy coverage and topography (Fig. 1). The Doon valley is surrounded by hills and includes a wide range of moist deciduous forest mainly dominated by Sal (*Shorea robusta*) stands in addition to a number of other woody species. Its climate is humid subtropical, with hot summers with temperatures of up to 36 °C and mild to warm winters with temperatures ranging between 5 and 23 °C (Peel et al., 2007). The region experiences five seasons during the year, spring (from mid-February to March), summer (from April to mid-June), monsoon period (from mid-June to mid-September), autumn (from mid-September to November), and winter (from December to mid-February). Annual rainfall is 2025 mm, most of which falls during the monsoon period. The region is partially affected by common lantana (*L. camara*), an invasive shrub that is extensively present in the western Himalayan forests in India (Khare et al., 2019a).

2.2. Datasets

2.2.1. Satellite data

We downloaded all available Landsat ETM + data (path 170 and row 55) with WRS-2 coordinates at L1T processing level and cloud cover below 70% from the USGS Glovis repository (http://glovis.usgs.gov) from 2000 to 2015 to form a dense time series. On average, 9 ETM + scenes were available per year until 2015, with fewer in 2000 and 2008 (Fig. 2). A total of 144 scenes were used for the analysis. The LEDAPS method (Masek et al., 2006), which is based on the 6S radiative transfer method (Vermote et al., 1997) was used to convert raw imagery from digital numbers (DNs) to Top of Atmosphere (ToA) and Surface (SR) reflectance. The pre-processed Landsat-7 data were acquired from USGS, which were later subject to generation of NDVI and MSAVI images using the surface reflectance values (Qi et al., 1994; Rouse et al., 1974).

2.2.2. Climate data

We used chronologies of temperature and precipitation from ERA-5 Monthly aggregates (5th generation) to explore the effect of environmental factors on Rao's Q diversity. This is a latest climate reanalysis produced by ECMWF (European Centre for Medium-Range Weather Forecasts) / Copernicus Climate Change Service (Škerlak et al., 2014),

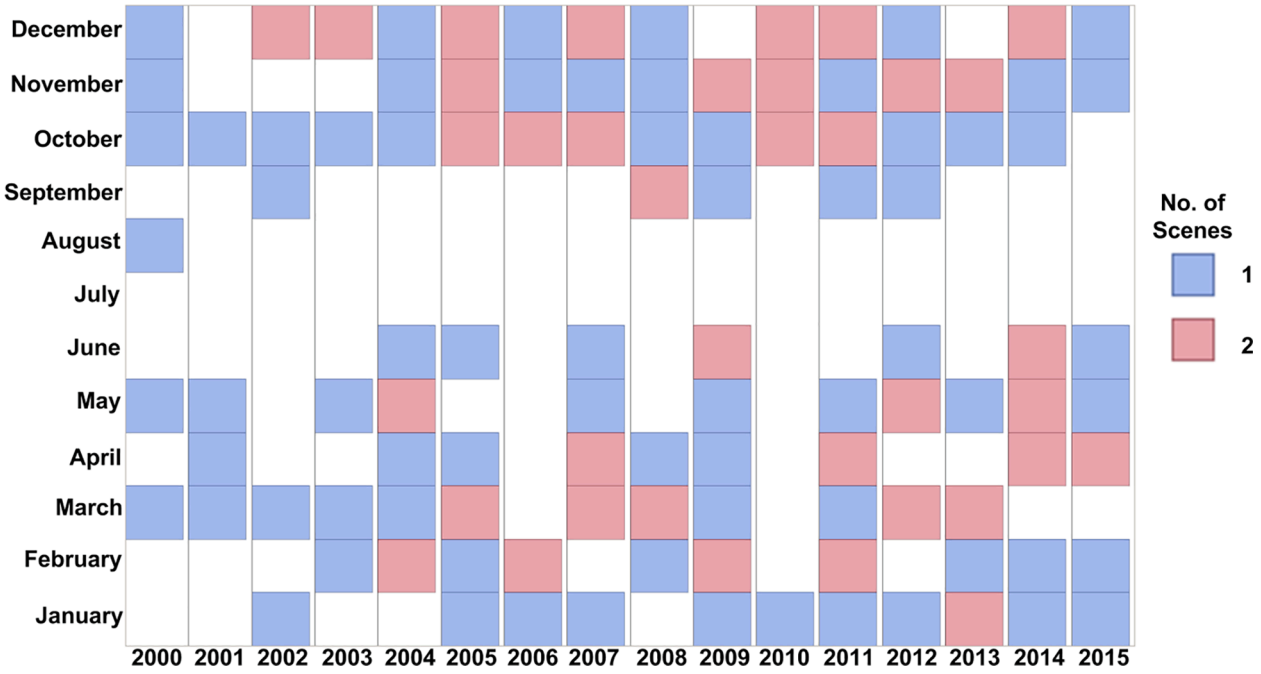

Fig. 2. Distribution of total 144 Landsat-7 ETM + scenes available from 2000 to 2015 for different months.

with a spatial resolution of 31 km. We selected atmospheric reanalysis data with total precipitation and near-surface temperature. This matched with the period of time series Landsat data. The ERA-5 data was extracted using Google Earth Engine (GEE) (https://earthengine.google.com/).

2.3. Time series analysis of Rao's Q diversity

NDVI and MSAVI were used as inputs for the estimation of Rao's Q diversity. NDVI is a conventional and widely used index for plant species diversity based on the difference between red and NIR domains of the electromagnetic spectrum (Arekhi et al., 2017; Rocchini et al., 2009b) according to the following equation:

$$NDVI = \frac{NIR - Red}{NIR + Red} \quad (1)$$

The MSAVI (Qi et al., 1994) was suggested to correct for the L factor of SAVI (Huete, 1988) and increased the signal-to-noise ratio of vegetation while minimizing the effect of soil background reflectance.

$$MSAVI = \frac{2*NIR + 1 - \sqrt{\left((2*NIR + 1)^2 - 8*(NIR - Red)\right)}}{2} \quad (2)$$

A fixed 3 × 3 – pixel window size was selected for index retrieval. The resolution was suggested as the optimal window size for optical image-based β-diversity assessment (Khare et al., 2019a). We adopted the spectralrao routine in R open source domain (R Core Team, 2017; Rocchini et al., 2017) for generation of time-series output images of Rao's Q diversity for NDVI (Q_{NDVI}) and MASVI (Q_{MSAVI}) respectively. Therefore, 144 raster images were generated separately for Q_{NDVI} and Q_{MSAVI}.

To understand the temporal variation in biodiversity from 2000 to 2015, mean values for NDVI, MSAVI, Q_{NDVI} and Q_{MSAVI} were computed for each raster image (i.e. 144 images) and parameters for a total of 576 images, using the routines implemented in R (Khare et al., 2017). Monthly averages of these data were plotted along with rainfall data to reflect the relationship of phenology with spectral heterogeneity derived β-diversity. Furthermore, we used these monthly time-series of Rao's Q diversity to derive annual coefficients of variation (CV_{annual}) for each year (2000 to 2015) using annualSummary routine implemented in bfastSpatial library in R (Verbesselt et al., 2010).

$$CV_{annual} = \frac{\sigma(Q_{timeseries})}{\mu(1 + Q_{timeseries})} \times 100 \quad (3)$$

Where $Q_{timeseries}$ represents the monthly time series Rao's Q raster images for respective years and σ ($Q_{timeseries}$), μ ($Q_{timeseries}$) denotes the standard deviation and mean value of monthly time series Rao's Q raster images for respective years. The CV_{annual} along the temporal gradient were calculated for each pixel in the annual Rao's Q diversity images and were further spatially mapped for both NDVI and MSAVI categories. We computed Pearson correlation coefficients between NDVI and MSAVI derived CV_{annual} for each year (Rodgers and Nicewander, 1988). We drew 100 training sample points within the study area for three classes representing three vegetation categories of agriculture, forest (sal-dominated) and invasive species (i.e. common lantana). The training points were generated from the available GPS observations during a field survey according to the procedure described in detail by Khare et al. (2019b).

2.4. Modelling environmental factors with Rao's Q and vegetation indices

Time series Rao's Q diversities from (Q_{NDVI} and Q_{MSAVI}) were modelled by multiple regressions as a function of vegetation indices (VIs) NDVI and MSAVI, and environmental factors including temperature (T_{mean}) and precipitation (PPT), according to their influence on vegetation response previously shown by Khare et al. (2017). A sensitivity analysis was performed using the standardized coefficients (Std. beta) of linear regressions as a direct measure of sensitivity to determine the specific contribution of environmental variables and vegetation indices on Rao's Q diversity (Ren et al., 2019).

2.5. Global sensitivity analysis

In addition, a variance-based global sensitivity analysis between Rao's Q diversity (Q_{NDVI} and Q_{MSAVI}) and vegetation indices (NDVI and MSAVI) was performed to compute first-order and total sensitivity indices (Saltelli, 2002) using Monte Carlo estimation of the Sobol' indices for a total number of $(p + 2) \times n$ model evaluations. Here, p represents number of random inputs ($p = 4$) and n represents the size of an initial Monte Carlo sample ($n = 10^5$). We adopted the sobol2002 routine of "sensitivity" library in R open source domain (Iooss et al., 2020).

2.6. Modelling Rao's Q diversity for vegetation classes

In order to understand the relationship between Q_{NDVI} and Q_{MSAVI} for the three vegetation classes, we calculated the CV of Rao's Q for each training point and modeled their relationship using the Generalized Linear Model (GLM) (Nelder and Wedderburn, 1972). We performed the GLM with identity link functions and normal distributed residuals for the response variable (Lopatin et al., 2016). The CV of Q_{MSAVI} and vegetation classes were used as explanatory variables in the model. The CV of Q_{NDVI} was used as response variable. In this analysis, Q_{NDVI} and Q_{MSAVI} are continuous variables, whereas the vegetation classes are categorical. Statistics were performed using JMP 14 (SAS institute Inc. 2018, Cary, NC).

3. Results

3.1. Comparison of index-based Rao's Q diversity

Overall, Rao's Q diversity varied from 0 to 0.05 (Fig. 3). It showed high values on agricultural land and sparse vegetation cover (>0.04), and varied topographically on mixed land use, which is attributed to combined spectral reflectance being received from agricultural land and sparse vegetation cover. Rao's Q diversity was lower (between 0.015 and 0.025) in the case of dense vegetation cover. It was attributed to spectral reflectance information received solely from overstory vegetation, which is dominated by one tree species (i.e. sal trees) resulting in lower spectral heterogeneity. Rao's Q of NDVI showed higher spatial variations compared to MSAVI, particularly for agricultural land and sparse vegetation cover, due to MSAVI ability to reduce the effect of soil and provide correct reflectance of agricultural land and sparse vegetation cover (Fig. 3a and b).

CV of Rao's Q diversity varied from 0 to 4 (Fig. 4). Temporal turnover of Rao's Q diversity derived from NDVI and MSAVI showed a different pattern among different sub-areas across the study site during 2000–2015. CV (Q_{NDVI}) showed higher temporal β –diversity than CV (Q_{MSAVI}) in areas with higher morphological landscape complexity shown by their spectral heterogeneity. However, CV (Q_{MSAVI}) was saturated when considering the temporal dimension compared to CV (Q_{NDVI}). In particular, agricultural land and sparse vegetation cover areas showed a lower relative value for MSAVI (between 0.75 and 1.25) compared to NDVI (between 1.75 and 2.75) (Fig. 4).

In addition, rainfall showed a culmination during the monsoon months (June to September), with a monthly average from June to September varying from 200 to 900 mm (Fig. 5). The average monthly vegetation index ranged from 0.62 to 0.88 for NDVI, and from 0.31 to 0.49 for MSAVI. Average monthly Rao's Q ranged between 0.02 and 0.035 for NDVI, and between 0.005 and 0.025 for MSAVI. Overall, the monthly trend of vegetation indices and Rao's Q diversity (Q_{NDVI} and Q_{MSAVI}) diverged between pre- and post-monsoon seasons, because of

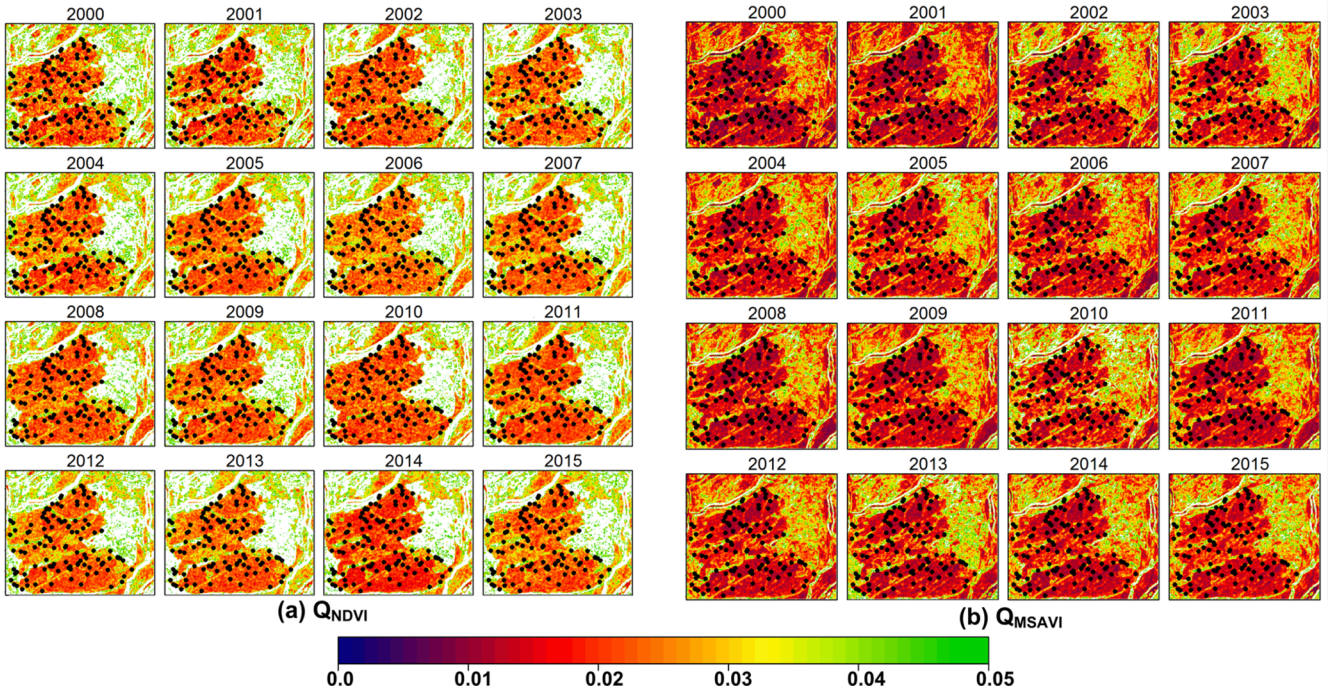

Fig. 3. Spatial representation of Rao's Q diversity derived from 2000 to 2015 for (a) NDVI and (b) MSAVI categories. Black points within each image represent the training datasets used in the analysis.

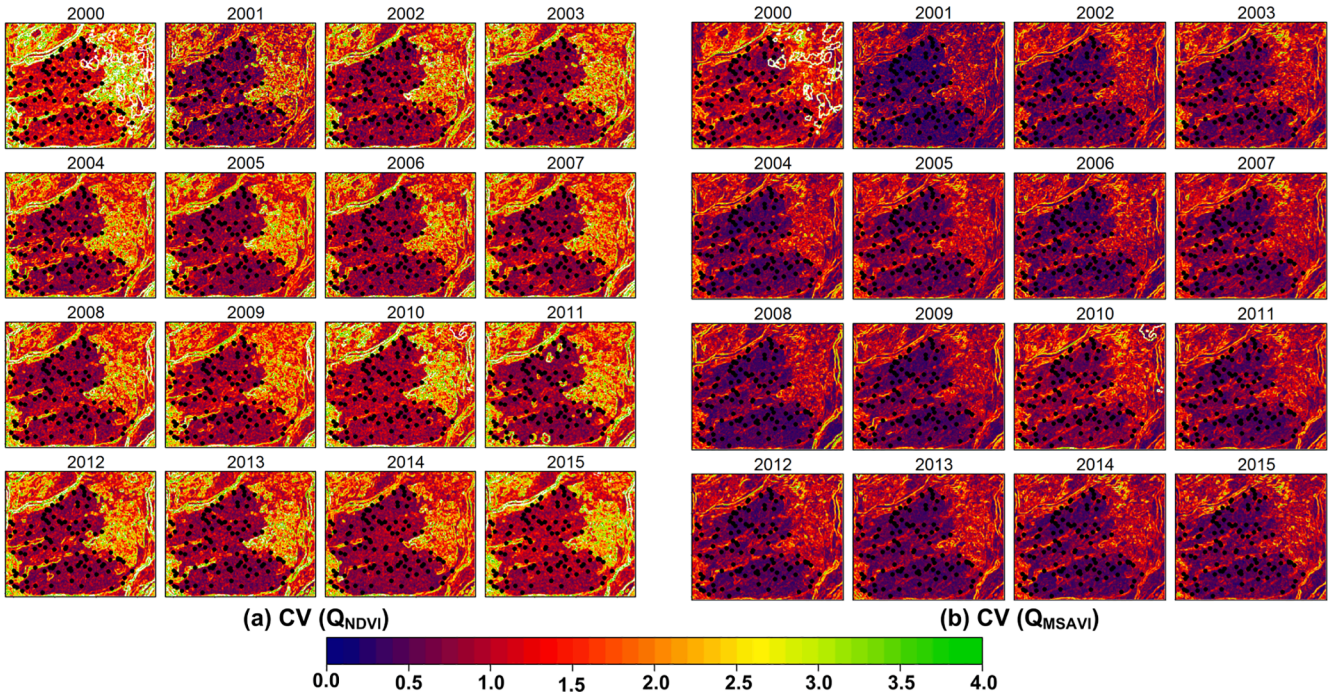

Fig. 4. Spatial representation of CV_{annual} (temporal turnover) of Rao's Q diversity derived from 2000 to 2015 for (a) NDVI and (b) MSAVI categories. Black points within each image represent the training datasets used in the analysis.

the site-specific precipitation regime with most rain fall occur between mid-June and the end of September (Fig. 5). In addition, the lack of optical satellite data during July and August due to cloud cover (Fig. 2) resulted in missing data, thus preventing the variability in vegetation index and Rao's Q diversity being exhaustively described during the monsoon season.

The vegetation indices-derived phenology showed an increasing greenness during the period between mid-monsoon (mid-June) and its end (September), followed by a decrease from mature leaf duration (winter months) to leaf fall stage (summer season). Q_{NDVI} and Q_{MSAVI} showed similar trends, reaching a minimum between June and October and increasing towards winter and spring, similar to the NDVI monthly variation. However, MSAVI monthly variations during winter were the opposite, which might be attributed to its reduced sensitivity to soil factors after the monsoon season.

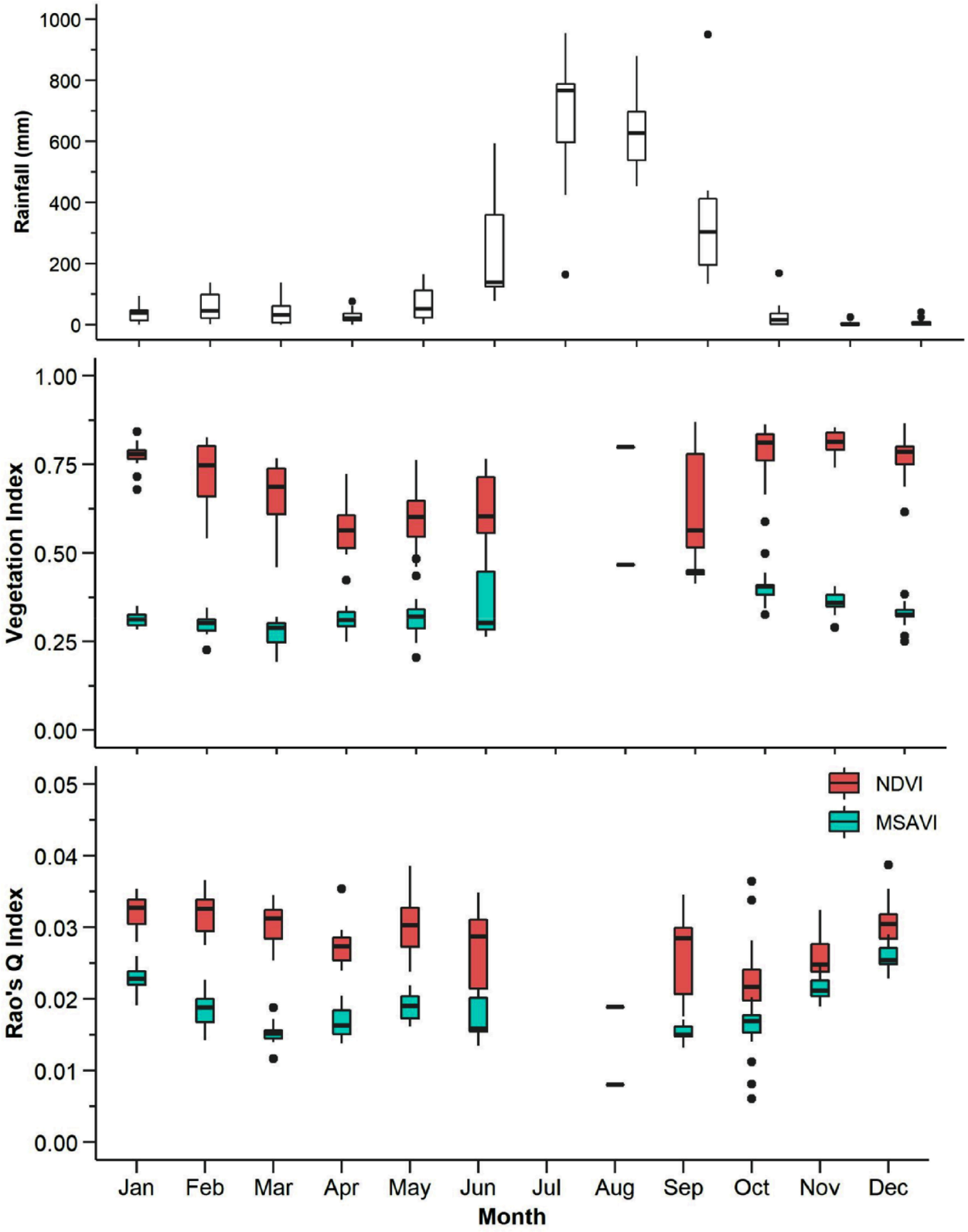

Fig. 5. Long-term monthly variations among vegetation indices, Rao's Q diversity index and rainfall from 2000 to 2015.

3.2. *Effect of temperature and precipitation on β-diversity*

Studentized residuals showed scatters of homoscedastic points and with a normal distribution of errors. Residuals showed no trend and some degree of unequal error variances, suggesting uncorrelated residuals and lack of outliers (Fig. 6).

Precipitation (Model I) and temperature (Model II) showed significant effects on Q_{MSAVI}, resulting in F value of 26.34 ($P < 0.0001$, $R^2 = 0.37$) and F value of 30.46 ($P < 0.0001$, $R^2 = 0.41$) respectively (Table 1). For Q_{MSAVI}, the sensitivity of temperature was higher (Std.

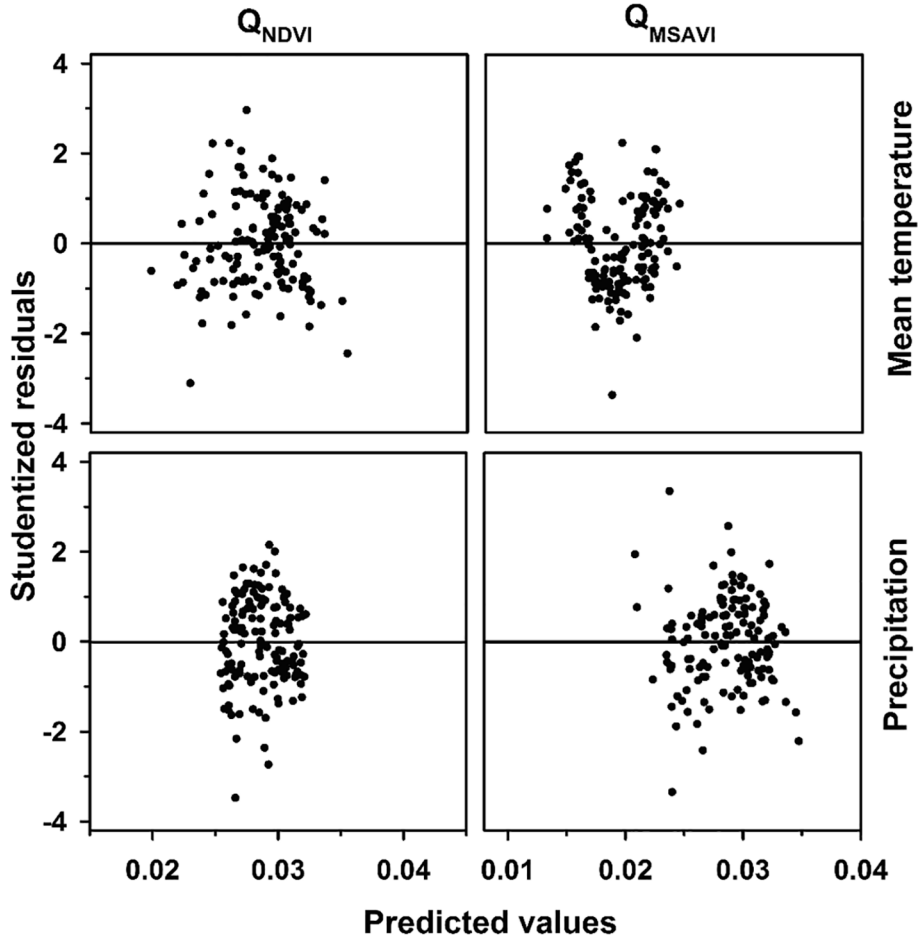

Fig. 6. Studentized residuals of the regression models performed between precipitation, temperature, NDVI, MSAVI and the Rao's Q diversity (Q_{NDVI} and Q_{MSAVI}).

Table 1
Statistical parameters (F, Std. beta and significance level $^{***}P < 0.0001$, $^{**}P < 0.01$ and $^{*}P < 0.05$) of linear mixed models based on Q_{NDVI}, Q_{MSAVI}, precipitation, temperature, NDVI and MSAVI).

Model	Response variable	Source of variation	Regressors		Overall model regressors	
			F-value	Absolute Std. Beta	F-value	R^2
Model I	Q_{MSAVI}	MSAVI	63.79^{**}	|0.551|	26.34^{***}	0.37
		PPT	9.01^{*}	|0.213|		
		MSAVI × PPT	4.42^{*}	|0.151|		
Model II	Q_{MSAVI}	MSAVI	8.01^{*}	|0.224|	30.46^{***}	0.41
		T_{mean}	89.29^{***}	|0.641|		
		MSAVI × T_{mean}	8.088	|0.224|		
Model III	Q_{NDVI}	NDVI	13.64^{**}	|0.305|	8.66^{***}	0.16
		PPT	6.96^{**}	|0.237|		
		NDVI × PPT	2.38	|0.133|		
Model IV	Q_{NDVI}	NDVI	53.16^{***}	|0.686|	27.41^{***}	0.38
		T_{mean}	54.31^{***}	|0.635|		
		NDVI × T_{mean}	1.84	|0.105|		

beta = 0.641) and the effects of the temperature were highly significant ($p < 0.0001$) when compared to the sensitivity and effects of precipitation (Std. beta = 0.213, $P < 0.05$) (Fig. 7; Table 1). The interaction between the temperature and MSAVI showed higher sensitivity (Std. beta = 0.224, $P < 0.05$) than interaction between the precipitation and MSAVI (Std. beta = 0.151, $P < 0.05$) (Fig. 7; Table 1).

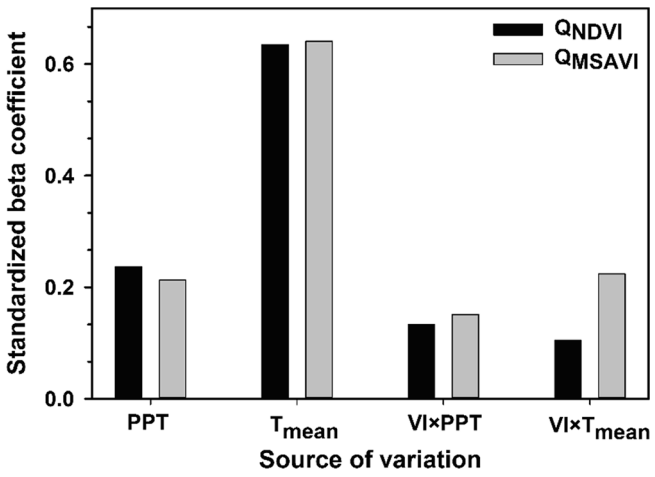

Fig. 7. Comparison of standardized beta coefficients of the regression models performed between precipitation (PPT), temperature (T_{mean}) and VI (NDVI and MSAVI) for Rao's Q diversity (Q_{NDVI} and Q_{MSAVI}).

For Q_{NDVI}, the sensitivity and effects of temperature was higher (Std. beta = 0.635, $P < 0.001$) than precipitation (Std. beta = 0.237, $P < 0.001$) (Fig. 7; Table 1). The interaction between the NDVI and temperature as well as the precipitation showed no significant influence. The effects of precipitation and temperature were reflected on Q_{NDVI}

(Model III and Model IV), but stronger and more significant was observed for temperature based Model IV (F value = 26.34, P < 0.0001 and R2 = 0.37) than precipitation based Model III (F value = 8.66, P < 0.0001and R^2 = 0.16).

3.3. Global sensitivity analysis of β-diversity and vegetation indices

The average value of Sobol' first order indices was 0.22 for different indices, with the minimum number recorded for Q_{NDVI}. The Sobol' first order indices varied between −0.17 to 0.54, with the maximum variation recorded for Q_{MSAVI}. The Q_{MSAVI} was characterized by the highest sensitivity and the maximum variation. The minimum difference was observed between vegetation indices NDVI and MSAVI (Fig. 8). In case of total sensitivity indices, an average value of 0.12 was observed, with the highest sensitivity and maximum variation recorded by Q_{MSAVI}. The minimum variations and lower sensitivity were observed for NDVI and MSAVI when compared to Rao's Q diversity (Fig. 8).

3.4. Relationship between Rao's Q diversity and vegetation classes

Compared with MSAVI, the NDVI-derived spatial Rao's Q showed higher values for the entire period (Fig. 9). Furthermore, CV was higher overall for NDVI-derived spatial Rao's Q across all three vegetation classes, compared with those derived from MSAVI. Among vegetation classes, agriculture showed higher variations than forest and lantana for both indices due to greater spectral variations (Fig. 10). However, forest class represented combinations of sal trees with some canopy gaps and understory vegetation, so sal-dominated forest showed higher CVs than areas colonized by a single plant species (lantana), which are mainly established in open areas, i.e. without overstory vegetation (Fig. 10). Results suggested a tendency for overestimation of diversity shown by

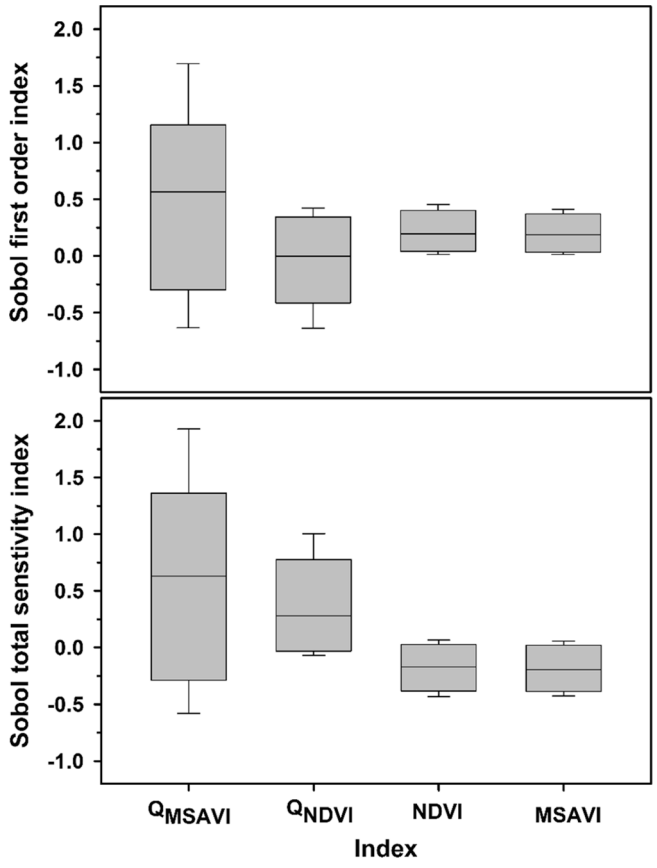

Fig. 8. Comparison of Sobol' based first order and total sensitivity indices between VI (NDVI and MSAVI) and Rao's Q diversity (Q_{NDVI} and Q_{MSAVI}).

overall higher mean values of temporal turnover from Q_{NDVI} than those from Q_{MSAVI} (Figs. 3 and 5). Generally, higher temporal turnovers in Q_{NDVI} and Q_{MSAVI} were detected in areas with mixed land use. The two indicators were shown to be variably correlated, with Pearson coefficients ranging between 0.022 in 2012 (p > 0.05) and 0.74 in 2001 (p < 0.001). The correlation coefficients in the other years were > 0.50 and highly significant (p < 0.001), except in 2002, 2003, 2010 and 2013 (Table 2).

The GLM produced a significant model with an F-value of 25.83 and P < 0.0001. Regressions were highly significant for both continuous (CV (Q_{MSAVI}); P < 0.0001) and categorical (vegetation classes; P < 0.001) variables along with their interaction (P < 0.05), with F-values ranging between 3.14 and 44.99 (Table 3). In general, 95% of data points exhibited studentized residuals of between −2 and 2 and were uniformly distributed around zero for all three vegetation classes (Fig. 11), suggesting that the analysis was properly represented by the model. The linear relationship of Rao's Q CV between NDVI and MSAVI showed highly significant correlations (P < 0.0001) for all three vegetation classes, which reduced from agriculture to forest and invasive species (Fig. 11).

4. Discussion

4.1. Observed β-diversity from Landsat data

In this paper, we tested the long-term time series spectral heterogeneity analysis in a biodiversity hotspot to estimate remote sensing β-diversity. We compared two different spectral indices of NDVI and MSAVI by deriving the Rao's Q diversity to monitor spectral heterogeneity changes over time for three land use classes. We calculated Rao's Q index for a rather smaller scale 3 × 3 window size for time series raster data, since it 1) takes both distance and relative abundance among pixels into account and 2) was previously shown to be superior to the traditional Shannon index for higher spatial resolutions (Khare et al., 2019a).

We tested the hypothesis that MSAVI-derived spatial Rao's Q provides higher spatial heterogeneity than NDVI but contrary to this our results showed that NDVI-derived spatial Rao's Q and temporal turnover showed overall higher values than those of MSAVI for different vegetation classes. This was attributed to the soil factor for which NDVI is more sensitive than MSAVI because the latter reduces the soil effect, which is found to have considerable impact on vegetation indices (Qi et al., 1994; Todd and Hoffer, 1998), especially in sparsely-vegetated and agricultural areas (Purevdorj et al., 1998). The annual CVs showed similar trends between NDVI and MSAVI based Rao's Q index for all vegetation classes, but with lower CVs for MSAVI compared to NDVI. Recent studies established the relationship between spectral reflectance-derived CV and spectral diversity for Rao's Q and Shannon indices (Khare et al., 2019a; Torresani et al., 2019). However, we extended this to deriving annual CVs from the time series Rao's Q raster images, which represent the temporal turnover of Rao's Q temporal diversity (Rocchini et al., 2019b). When discussing major biodiversity trends, Mcgill et al. (2015) also considered the importance of temporal β diversity being investigated on multiple spatial scales, such as local, *meta*-community, bio-geographical, and global. Here, we followed a local-scale approach to present our workflow for multi-date spatiotemporal analysis of spectral turnover. However, this approach can feasibly be generalized to larger scales, particularly thanks to its broad independence from field observations and the availability of openly accessible remote sensing data sources.

Convertino et al., (2012) proposed Kullback-Leibler (KL) divergence algorithm for β-diversity estimation compared with traditional Shannon entropy approach derived from Landsat-RGB bands as spectral signature of temporal heterogeneity of the landscape for soil, vegetation and water. They indicated that the performance of KL divergence is more significant than conventional Shannon entropy algorithm. In this study, we used Rao's Q index as an innovative measure of spectral variation

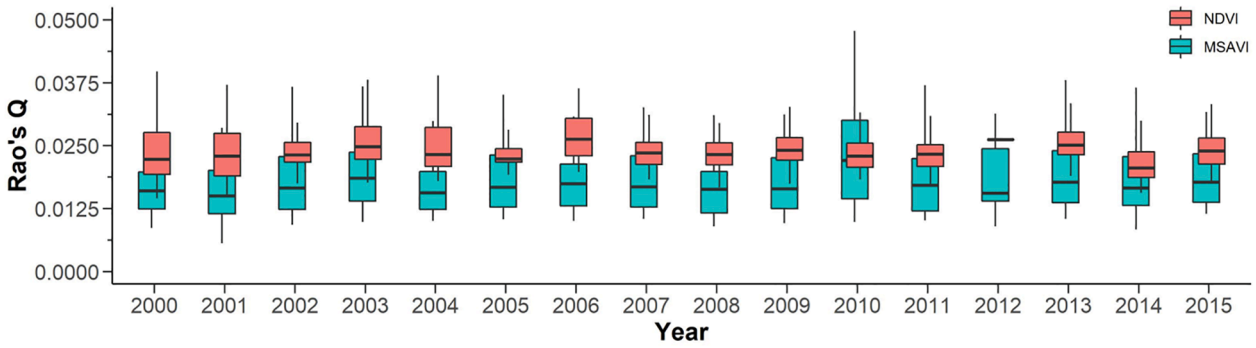

Fig. 9. Rao's Q diversity values derived by NDVI and MSAVI calculated for the 16 study.

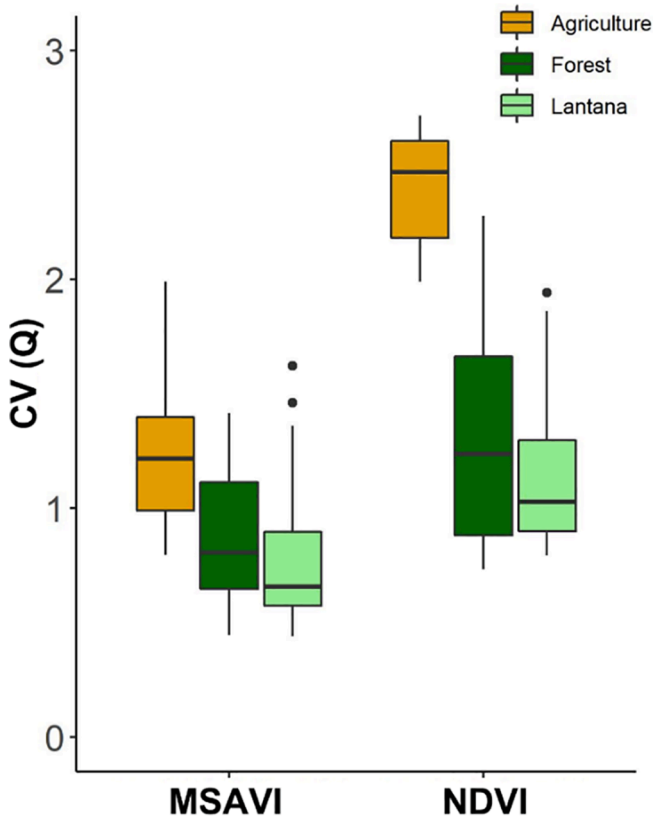

Fig. 10. CV derived from Rao's Q calculated from NDVI and MSAVI for different vegetation classes.

Table 2
Correlation coefficients between NDVI and MSAVI derived CV_{annual}. Three asterisks indicate $p < 0.001$.

Year	r
2000	0.69***
2001	0.74***
2002	0.41***
2003	0.49***
2004	0.71***
2005	0.50***
2006	0.58***
2007	0.57***
2008	0.50***
2009	0.61***
2010	0.28***
2011	0.57***
2012	0.02
2013	0.49***
2014	0.60***
2015	0.57***

Table 3
Results from the GLM evaluating the relationship between CV (Q_{NDVI}) and CV (Q_{MSAVI}) for different vegetation classes.

Source of variation	Regressors			Model		
	Type III SS	F-value	P	F-value	P	R^2
CV (Q_{MSAVI})	20.89	44.99	<0.0001	25.83	<0.0001	0.62
class	8.51	9.16	<0.001			
CV (Q_{MSAVI}) × class	2.92	3.14	<0.05			

hypothesis (SVH) in remote sensing (Rocchini et al., 2017), which accounts for both the abundance and the pairwise spectral distance among pixels. We derived time series Rao's Q index using two different spectral indices of NDVI and MSAVI that incorporate NIR (770–900 nm) and red bands (630–690 nm) as two photosynthetically crucial spectral domains that are useful for determining different types of species and plant stress (Gamon et al., 1995; Grace et al., 2007). To the best of our knowledge, this is the first study that compares two vegetation indices to test the relationship of spectral heterogeneity across three different vegetation classes (forest, invasive species and agriculture land), and compare their sensitivity for environmental factors (temperature and precipitation) to measure SVH derived from Rao's Q index. Another important aspect is to the effect of combined reflectance from soil and vegetation on NDVI and MSAVI (Qi et al., 1994). Our results suggested that both indices affect the spectral heterogeneity information derived from remote sensing imagery (Rocchini, 2007; Tuomisto et al., 2003). Future studies should focus on other multi-spectral vegetation indices-diversity relationships, including those extracted from red-edge bands, since they enable recording even subtle differences in leaf structure and chlorophyll content (Delegido et al., 2011; Schuster et al., 2012).

4.2. Seasonal and temporal analysis of β-diversity

This study demonstrated that the relationship between vegetation index-derived spectral variability and species diversity changes during the year. A previous study in moist deciduous forests showed the association between Rényi diversity and NDVI anomalies during pre- and post-monsoon season, with less spectral heterogeneity for dense cover areas (in which understory vegetation is not visible) and maximum spectral reflectance observed from overstory vegetation (dominated by dense sal trees) (Khare et al., 2018). Environmental factors such as temperature and precipitation influence β-diversity of the MDF, which can be reflected by vegetation indices like NDVI and MSAVI. Sensitivity analysis revealed that the relative significances of the indices and

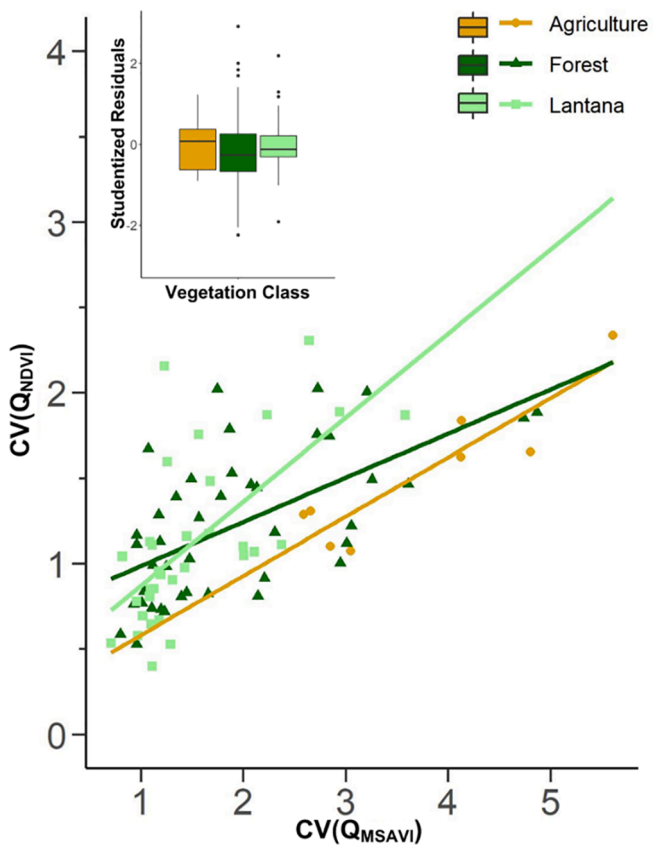

Fig. 11. Relationship between CV (Q_{NDVI}) and CV (Q_{MSAVI}) for the three vegetation classes.

environmental factors as main effects were higher than their interaction. Parameter estimation suggests that the likelihood of Rao's Q diversity is more sensitive to temperature compared to precipitation for both indices. A former analysis in a similar area showed that the temperature and precipitation were strongly correlated with NDVI and played major role in changes in vegetation greenness in MDF (Khare et al., 2017). Furthermore, an analysis in water conservation area showed that the Landsat RGB based β-diversity are strongly correlated with changes in vegetation composition and the average annual rainfall of each season (Convertino et al., 2012). Other studies also observed a significant relationship of NDVI with tree species diversity, species composition and plant richness for varying seasons (Levin et al., 2007; Madonsela et al., 2017; Schmidtlein and Fassnacht, 2017; Torresani et al., 2019). Moreover, the moist deciduous forest in the study site was mainly dominated by sal trees, which experience drastic seasonal changes with their leaf fall (January to mid-March), leaf flush (mid-March to September) and mature leaf (October to December) phenological phases. This seasonal transition resulted in a strong variability of spectral reflectance (Khare et al., 2017). As a consequence, spectral heterogeneity changes with seasons. Our results agreed with previous studies, which showed a significant relationship between vegetation indices and Rao's Q diversity. In particular, Rao's Q diversity was shown to increase along with the changes from pre- to post-monsoon seasons, with increase in the vegetation greenness.

Previous studies reported that the spectral heterogeneity derived from Rao's Q diversity is scale and sensor dependent, and estimating species diversity could be improved at higher spatial resolutions (Khare et al., 2019a; Torresani et al., 2019). Recently, Torresani et al. (2019) applied a two-year collection of Sentinel-2 optical data (10 m spatial resolution) and showed that Rao's Q diversity data was highly correlated with field heterogeneity compared to medium spatial resolution Landsat-8 (30 m) data. However, the still short period of Sentinel data availability eventually limits it capabilities when long-term analysis is required. This gap could be filled by other openly-available data from Landsat and MODIS archives (available from 1972 and 2000 onwards), yet at lower spatial resolutions of 30 m and 250 m, respectively.

The basic principles of generalizing optical remote sensing based β-diversity measures to multi-temporal domain has recently been presented by Rocchini et al. (2019b) using coarse spatial resolution MODIS time series. Therefore, we applied time series of Landsat data for a 15-year period over a mountainous biodiversity hotspot, to extend β-diversity analysis at wider spatial resolutions for supporting regional- to landscape- level assessments. This was also partially motivated by recent studies on the moist deciduous forest site in which a multi-resolution framework was proposed to assess diversity indicators using high spatial resolution data but short time windows (Khare et al., 2019a). Integration of abiotic environmental variables into modelling of β -diversity patterns is urgently required, having been suggested to be potentially advantageous for studies on remote sensing-assisted prediction of biodiversity changes (Ferrier et al., 2017). We applied this by jointly considering monthly rainfall with temporal variation of Rao's Q from both vegetation indices, which enables to distinguish between pre- and post- monsoon seasons as well as to further interpret temporal turnover of diversity with respect to seasonality.

We showed significance of vegetation indices and β-diversity estimations on an inter-annual basis for all months except July and August, which was attributed to constrained availability of cloud-free optical imageries during the monsoon period, resulting in substantial loss of information during that time. This major drawback of passive optical imagery, namely their infeasibility to overcome atmospheric obstacles, thus hindered a full collection of Landsat scenes during the monsoon period. Hence, strategies for either enriching or gap-filling of optical time series with open-access SAR imagery (like Sentinel-1) or solely temporal analysis based on SAR data should be amongst the main focuses for future research on multi-date biodiversity assessments using remote sensing data. A very recent communication published by Bae et al. (2019) touched on this topic in a multi-temporal context by an analysis of SAR data predictive performance on vegetation structure and species composition of birds and beetles, and provided further advice on how Sentinel-1 data could offer alternatives for modelling biodiversity (α, β and γ) of different functional groups.

In the past decades, the SVH was tested using several new spectral heterogeneity based indices with different remote sensing data for different ecosystems and proposed time series approach has successfully provided space and time relationship of spectral and field diversity (Skidmore et al., 2015; Zellweger et al., 2019). We are aware that further tests should be conducted in different environments for the assessment of biodiversity quality attributes suggested by (Feest et al., 2010). The biodiversity quality and pattern may vary in different sites, and if comprehensive data on species richness and abundances is available then this data could be combined with different indicators (vegetation biomass, species value index and density) and remote sensing derived indices (Feest et al., 2010; Jalkanen et al., 2020).

4.3. *β-diversity for different vegetation classes*

This study suggested the usefulness of optical data time series for estimation of species diversity across different vegetation classes based on significant relationships between vegetation indices and β-diversity. Vegetation indices provide spectral content from vegetation by suppressing spectral reflectance from non-vegetative features such as soil, water and built-up features (Huete et al., 2002; Viña et al., 2011). In this study, CVs of β- diversity were significantly correlated for all three vegetation classes for both NDVI and MSAVI, which implies that the variability in vegetation type characteristics is highly related to spectral heterogeneity caused by species diversity (Rocchini et al., 2010). However, NDVI showed higher temporal turnover of β- diversity compared to MSAVI for all three land use classes, which suggests

differences in sensitivity between vegetation indices resulting from variability in vegetation characteristics (Madonsela et al., 2017). One possible explanation for this difference is due to higher sensitivity of NDVI to soil background compared to MSAVI, which uses the soil factor to reduce the effect of soil on vegetation characteristics (Qi et al., 1994; Todd and Hoffer, 1998).

Assimilation of field and remote sensing data for biodiversity assessment faces serious challenges if the optical remote sensing data is unable to identify biodiversity or ecological traits, in particular for species- or genetic-level attributes, and also underpins the potentials of linking α and β diversities to land use and its changes via modeling at grid cell level in an earth observation context (Ferrier et al., 2017). Integration of β diversity and remotely-sensed environmental change with either discrete classes (e.g. land use or vegetation types) or continuous patterns has also been suggested by Ferrier (2011), with interesting implications in quantifying and understanding the effects of habitat loss on biodiversity conservation. Our study provided the fundamental basis to understand the relationship between β diversity and spectral variability for different land use, which in turn may be used as a proxy for species diversity in space and time for different ecosystems.

5. Conclusion

In this study, we estimated spatio-temporal β-diversity using time series vegetation indices derived Raós Q index. To the best of our knowledge, it is the first time the ability has been tested of multi-temporal Raós Q derived from two vegetation indices (MSAVI and NDVI), and effect of environmental factors (temperature and precipitation), to quantify the spatiotemporal diversities across major humid sub-tropical land use types with different properties, including an endemic forest type and areas colonized by an invasive species. The results showed how the Rao's Q diversities and their temporal turnover can distinguish between land use types as well as pre- and post-monsoon over an entire 15-year period, and can therefore be a further indication of the applicability of spectral heterogeneity information for β-diversity analysis in a real-world example. In addition, and somewhat in contrary to our prior hypothesis, NDVI-derived spatial Rao's Q and temporal turnover showed overall higher values than those of MSAVI, which suggests a tendency towards overestimation due to higher sensitivity of NDVI to soil backgrounds. However, MSAVI derived Rao's Q index showed higher sensitivity towards environmental factors compared to NDVI. We demonstrated that the estimated diversity changes with seasonality and vegetation greenness, and our results indicated that there is significant transition in β-diversity values during pre- and post-monsoon seasons. The observed spectral heterogeneity, especially in heterogeneous agricultural land use, was successfully distinguished from forest and lantana classes. This approach can be used for monitoring long-term forest diversity disturbances at wide geographical scale, and enable new applications to explore the Landsat data archive in the prediction of biodiversity variations over time. This study included two mostly used vegetation indices. However, questions still remain, such as the temporal effect of other vegetation indices involving different spectral ranges such as blue, red-edge, narrow near infrared and short wave infrared.

CRediT authorship contribution statement

Siddhartha Khare: Conceptualization, Methodology, Software, Data curation, Writing - original draft, Writing - review & editing, Visualization. **Hooman Latifi:** Conceptualization, Writing - original draft, Writing - review & editing, Supervision. **Sergio Rossi:** Writing - review & editing, Supervision, Funding acquisition.

Declaration of Competing Interest

The authors declare that they have no known competing financial interests or personal relationships that could have appeared to influence the work reported in this paper.

Acknowledgements

The data used within this research were partially provided by U.S. Geological Survey (USGS) EROS data center and Copernicus Climate Change Service (C3S). We thank A. Garside for checking the English text. The authors thank the reviewers for providing their constructive comments on the manuscript, which notably improved the paper.

Funding

This research received no external funding.

Author contributions

S.K., and H.L., designed the research. S.K. conducted the data processing, coding, result preparation and analysis. S.K., and H.L., performed the statistical interpretation. S.K. and H.L. wrote the first draft of paper together. H.L., and S.R. commented on the draft and all authors finalized it. S.R. provided the research funding for the first author at University of Quebec in Chicoutimi (UQAC), Canada. S.K. was the corresponding author.

Appendix A. Supplementary data

Supplementary data to this article can be found online at https://doi.org/10.1016/j.ecolind.2020.107105.

References

Arekhi, M., Yılmaz, O.Y., Yılmaz, H., Akyüz, Y.F., 2017. Can tree species diversity be assessed with Landsat data in a temperate forest? Environ. Monit. Assess. https://doi.org/10.1007/s10661-017-6295-6.

Bae, S., Levick, S.R., Heidrich, L., Magdon, P., Leutner, B.F., Wöllauer, S., Serebryanyk, A., Nauss, T., Krzystek, P., Gossner, M.M., Krah, F., Culmsee, H., Jung, K., Heurich, M., Fischer, M., 2019. Radar vision in the mapping of forest biodiversity from space. Nat. Commun. 10, 4757. https://doi.org/10.1038/s41467-019-12737-x.

Convertino, M., Mangoubi, R.S., Linkov, I., Lowry, N.C., Desai, M., 2012. Inferring species richness and turnover by statistical multiresolution texture analysis of satellite imagery. PLoS One 7. https://doi.org/10.1371/journal.pone.0046616.

Delegido, J., Verrelst, J., Alonso, L., Moreno, J., 2011. Evaluation of sentinel-2 red-edge bands for empirical estimation of green LAI and chlorophyll content. Sensors 11, 7063–7081. https://doi.org/10.3390/s110707063.

Feest, A., Aldred, T.D., Jedamzik, K., 2010. Biodiversity quality: A paradigm for biodiversity. Ecol. Indic. 10, 1077–1082. https://doi.org/10.1016/j.ecolind.2010.04.002.

Ferrier, S., 2011. Extracting more value from biodiversity change observations through integrated modeling. Bioscience 61, 96–97. https://doi.org/10.1525/bio.2011.61.2.2.

Ferrier, S., Jetz, W., Scharlemann, J., 2017. Biodiversity modelling as part of an observation system á modelling á monitoring á, in: scholes, M.W. and R.J. (Ed.), The GEO Handbook on Biodiversity Observation Networks. Springer, Cham, pp. 239–326. https://doi.org/10.1007/978-3-319-27288-7_10.

Gamon, J.A., Field, C.B., Goulden, M.L., Griffin, K.L., Hartley, A.E., Joel, G., Penuelas, J., Valentini, R., 1995. Relationships between NDVI, canopy structure, and photosynthesis in three California vegetation types. Ecol. Appl. 5, 28–41.

Gillespie, T.W., Foody, G.M., Rocchini, D., Giorgi, A.P., Saatchi, S., 2008. Measuring and modelling biodiversity from space. Prog. Phys. Geogr. https://doi.org/10.1177/0309133308093606.

Grace, J., Nichol, C., Disney, M., Lewis, P., Quaife, T., Bowyer, P., 2007. Can we measure terrestrial photosynthesis from space directly, using spectral reflectance and fluorescence? Glob. Chang. Biol. 13, 1484–1497. https://doi.org/10.1111/j.1365-2486.2007.01352.x.

Hernández-Stefanoni, J.L., Gallardo-Cruz, J.A., Meave, J.A., Rocchini, D., Bello-Pineda, J., López-Martínez, J.O., 2012. Modeling α- and β-diversity in a tropical forest from remotely sensed and spatial data. Int. J. Appl. Earth Obs. Geoinf. 19, 359–368. https://doi.org/10.1016/j.jag.2012.04.002.

Huete, A.R., 1988. A Soil-Adjusted Vegetation Index (SAVI). Remote Sens. Environ. 25, 295–309. https://doi.org/10.1016/0034-4257(88)90106-X.

Huete, A., Didan, K., Miura, T., Rodriguez, E., Gao, X., Ferreira, L., 2002. Overview of the radiometric and biophysical performance of the MODIS vegetation indices. Remote Sens. Environ. 83, 195–213. https://doi.org/10.1016/S0034-4257(02)00096-2.

Iooss, B., Da Veiga, S., Janon, A., Pujol, G., Iooss, M.B., Rcpp, L., Suggests condMVNorm, R., DiceDesign, D., 2020. Package 'sensitivity.'.

Jalkanen, J., Vierikko, K., Moilanen, A., 2020. Spatial prioritization for urban Biodiversity Quality using biotope maps and expert opinion. Urban For. Urban Green. 49, 126586 https://doi.org/10.1016/j.ufug.2020.126586.

Khare, S., Ghosh, S.K., Latifi, H., Vijay, S., Dahms, T., 2017. Seasonal-based analysis of vegetation response to environmental variables in the mountainous forests of western himalaya using landsat 8 data. Int. J. Remote Sens. 38 https://doi.org/10.1080/01431161.2017.1320450.

Khare, S., Latifi, H., Ghosh, S.K., 2018. Multi-scale assessment of invasive plant species diversity using Pléiades 1A, RapidEye and Landsat-8 data. Geocarto Int. 33, 681–698. https://doi.org/10.1080/10106049.2017.1289562.

Khare, S., Latifi, H., Rossi, S., 2019a. Forest beta-diversity analysis by remote sensing: How scale and sensors affect the Rao's Q index. Ecol. Indic. 106, 105520 https://doi.org/10.1016/j.ecolind.2019.105520.

Khare, S., Latifi, H., Rossi, S., Ghosh, S.K., 2019b. Fractional cover mapping of invasive plant species by combining very high-resolution stereo and multi-sensor multispectral imageries. Forests 10, 1–15. https://doi.org/10.3390/f10070540.

Kissling, W.D., Ahumada, J.A., Bowser, A., Fernandez, M., Fernández, N., García, E.A., Guralnick, R.P., Isaac, N.J.B., Kelling, S., Los, W., McRae, L., Mihoub, J.B., Obst, M., Santamaria, M., Skidmore, A.K., Williams, K.J., Agosti, D., Amariles, D., Arvanitidis, C., Bastin, L., De Leo, F., Egloff, W., Elith, J., Hobern, D., Martin, D., Pereira, H.M., Pesole, G., Peterseil, J., Saarenmaa, H., Schigel, D., Schmeller, D.S., Segata, N., Turak, E., Uhlir, P.F., Wee, B., Hardisty, A.R., 2018. Building essential biodiversity variables (EBVs) of species distribution and abundance at a global scale. Biol. Rev. 93, 600–625. https://doi.org/10.1111/brv.12359.

Lausch, A., Bannehr, L., Beckmann, M., Boehm, C., Feilhauer, H., Hacker, J.M., Heurich, M., Jung, A., Klenke, R., Neumann, C., Pause, M., Rocchini, D., Schaepman, M.E., Schmidtlein, S., Schulz, K., Selsam, P., Settele, J., Skidmore, A.K., Cord, A.F., 2016. Linking earth observation and taxonomic, structural and functional biodiversity: Local to ecosystem perspectives. Ecol. Indic. 70, 317–339. https://doi.org/10.1016/j.ecolind.2016.06.022.

Levin, N., Shmida, A., Levanoni, O., Tamari, H., Kark, S., 2007. Predicting mountain plant richness and rarity from space using satellite-derived vegetation indices. Divers. Distrib. 13, 692–703. https://doi.org/10.1111/j.1472-4642.2007.00372.x.

Lopatin, J., Dolos, K., Hernández, H.J., Galleguillos, M., Fassnacht, F.E., 2016. Comparing generalized linear models and random forest to model vascular plant species richness using LiDAR data in a natural forest in central Chile. Remote Sens. Environ. 173, 200–210. https://doi.org/10.1016/j.rse.2015.11.029.

Madonsela, S., Cho, M.A., Ramoelo, A., Mutanga, O., 2017. Remote sensing of species diversity using Landsat 8 spectral variables. ISPRS J. Photogramm. Remote Sens. https://doi.org/10.1016/j.isprsjprs.2017.10.008.

Masek, J.G., Vermote, E.F., Saleous, N.E., Wolfe, R., Hall, F.G., Huemmrich, K.F., Gao, F., Kutler, J., Lim, T.K., 2006. A landsat surface reflectance dataset for North America, 1990–2000. IEEE Geosci. Remote Sens. Lett. 3, 68–72. https://doi.org/10.1109/LGRS.2005.857030.

Mcgill, B.J., Dornelas, M., Gotelli, N.J., Magurran, A.E., 2015. Fifteen forms of biodiversity trend in the Anthropocene. Trends Ecol. Evol. 30, 104–113. https://doi.org/10.1016/j.tree.2014.11.006.

Nelder, A.J.A., Wedderburn, R.W.M., 1972. Generalized linear models. J. R. Stat. Soc. Ser. A 135, 370–384. https://doi.org/10.2307/2344614.

Palmer, M.W., Earls, P.G., Hoagland, B.W., White, P.S., Wohlgemuth, T., 2002. Quantitative tools for perfecting species lists. Environmetrics 13, 121–137. https://doi.org/10.1002/env.516.

Peel, M.C., Finlayson, B.L., McMahon, T.A., 2007. World map of the Köppen-Geiger climate classification updated. Meteorol. Zeitschrift 15, 259–263. https://doi.org/10.1127/0941-2948/2006/0130.

Purevdorj, T., Tateishi, R., Ishiyama, T., Honda, Y., 1998. Relationships between percent vegetation cover and vegetation indices. Int. J. Remote Sens. 19, 3519–3535. https://doi.org/10.1080/014311698213795.

Qi, J., Chehbouni, A., Huete, A.R., Kerr, Y.H., Sorooshian, S., 1994. A Modified Soil Adjusted Vegetation Index. Remote Sens. Environ. 48, 119–126. https://doi.org/10.1016/0034-4257(94)90134-1.

R Core Team, 2017. R: A language and environment for statistical computing. http://www.R-project.org/. [WWW Document]. R Found. Stat. Comput. Vienna, Austria.

Rao, C.R., 1982. Diversity and dissimilarity coefficients: A unified approach. Theor. Popul. Biol. 21, 24–43. https://doi.org/10.1016/0040-5809(82)90004-1.

Ren, P., Ziaco, E., Rossi, S., Biondi, F., Prislan, P., Liang, E., 2019. Growth rate rather than growing season length determines wood biomass in dry environments. Agric. For. Meteorol. 271, 46–53. https://doi.org/10.1016/j.agrformet.2019.02.031.

Rocchini, D., 2007. Distance decay in spectral space in analysing ecosystem β-diversity. Int. J. Remote Sens. 28, 2635–2644. https://doi.org/10.1080/01431160600954712.

Rocchini, D., Balkenhol, N., Carter, G.A., Foody, G.M., Gillespie, T.W., He, K.S., Kark, S., Levin, N., Lucas, K., Luoto, M., Nagendra, H., Oldeland, J., Ricotta, C., Southworth, J., Neteler, M., 2010. Remotely sensed spectral heterogeneity as a proxy of species diversity: Recent advances and open challenges. Ecol. Inform. 5, 318–329. https://doi.org/10.1016/j.ecoinf.2010.06.001.

Rocchini, D., He, K.S., Zhang, J., 2009a. Is spectral distance a proxy of beta diversity at different taxonomic ranks? A test using quantile regression. Ecol. Inform. https://doi.org/10.1016/j.ecoinf.2009.07.001.

Rocchini, D., Marcantonio, M., Da, D., Chirici, G., Galluzzi, M., Lenoir, J., Ricotta, C., Torresani, M., Ziv, G., 2019b. Time-lapsing biodiversity: An open source method for measuring diversity changes by remote sensing. Remote Sens. Environ. 231, 111192 https://doi.org/10.1016/j.rse.2019.05.011.

Rocchini, D., Marcantonio, M., Ricotta, C., 2017. Measuring Rao's Q diversity index from remote sensing: An open source solution. Ecol. Indic. 72, 234–238. https://doi.org/10.1016/j.ecolind.2016.07.039.

Rocchini, D., Wohlgemuth, T., Ricotta, C., Ghisleni, S., Stefanini, A., Chiarucci, A., 2009b. Rarefaction theory applied to satellite imagery for relating spectral and species diversity. Riv. Ital. di Telerilevamento 41, 109–123. https://doi.org/10.5721/ItJRS20094128.

Rodgers, J.L., Nicewander, W.A., 1988. Thirteen ways to look at the correlation coefficient. Am. Stat. 42, 59–66. https://doi.org/10.1080/00031305.1988.10475524.

Rouse, W., Haas, H., Deering, W., 1974. 20 Monitoring vegetation systems in the great plains with Erts. Proc. Third ERTS Symp. 309–317.

Saltelli, A., 2002. Making best use of model evaluations to compute sensitivity indices. Comput. Phys. Commun. 145, 280–297. https://doi.org/10.1016/S0010-4655(02)00280-1.

Schmidtlein, S., Fassnacht, F.E., 2017. The spectral variability hypothesis does not hold across landscapes. Remote Sens. Environ. 192, 114–125. https://doi.org/10.1016/j.rse.2017.01.036.

Schuster, C., Förster, M., Kleinschmit, B., 2012. Testing the red edge channel for improving land-use classifications based on high-resolution multi-spectral satellite data. Int. J. Remote Sens. 33, 5583–5599. https://doi.org/10.1080/01431161.2012.666812.

Škerlak, B., Sprenger, M., Wernli, H., 2014. A global climatology of stratosphere-troposphere exchange using the ERA-Interim data set from 1979 to 2011. Atmos. Chem. Phys. 14, 913–937. https://doi.org/10.5194/acp-14-913-2014.

Skidmore, A.K., Pettorelli, N., Coops, N.C., Geller, G.N., Hansen, M., Lucas, R., Mücher, C.A., O'Connor, B., Paganini, M., Henrique Miguel Pereira, Michael E. Schaepman, W.T., Wang, T., Wegmann, M., 2015. Agree on biodiversity metrics to track from space. Nature 523, 5–7. https://doi.org/10.1038/523403a.

SAS Institute Inc., 2018. Discovering JMP 14®. Cary, NC: SAS Institute Inc.

Todd, S.W., Hoffer, R.M., 1998. Responses of spectral indices to variations in vegetation cover and soil background. Photogramm. Eng. Remote Sens. 64, 915–922.

Torresani, M., Rocchini, D., Sonnenschein, R., Zebisch, M., Marcantonio, M., Ricotta, C., Tonon, G., 2019. Estimating tree species diversity from space in an alpine conifer forest: The Rao's Q diversity index meets the spectral variation hypothesis. Ecol. Inform. 52, 26–34. https://doi.org/10.1016/j.ecoinf.2019.04.001.

Tuomisto, H., Ruokolainen, K., Yli-Halla, M., 2003. Dispersal, environment, and floristic variation of Western Amazonian forests. Science 299, 241–244. https://doi.org/10.1126/science.1078037.

Verbesselt, J., Hyndman, R., Newnham, G., Culvenor, D., 2010. Detecting trend and seasonal changes in satellite image time series. Remote Sens. Environ. 114, 106–115. https://doi.org/10.1016/j.rse.2009.08.014.

Vermote, E.F., Tanr, D., Deuz, J.L., Herman, M., Morcrette, J., 1997. Second simulation of the satellite signal in the solar spectrum, 6S : An Overview. IEEE Trans. Geosci. Remote Sens. 35, 675–686.

Vihervaara, P., Auvinen, Ari-Pekka, Mononen, Laura, Törmä, Markus, Ahlroth, Petri, Anttila, Saku, Böttcher, Kristin, Forsius, Martin, Heino, Jani, Heliölä, Janne, Koskelainen, Meri, Kuussaari, Mikko, Meissner, Kristian, Ojala, Olli, Tuominen, Seppo, Viitasalo, Markku, Virkkala, R., 2017. How essential biodiversity variables and remote sensing can help national biodiversity monitoring. Glob. Ecol. Conserv. 10, 43–59. https://doi.org/10.1016/j.gecco.2017.01.007.

Viña, A., Gitelson, A.A., Nguy-robertson, A.L., Peng, Y., 2011. Comparison of different vegetation indices for the remote assessment of green leaf area index of crops. Remote Sens. Environ. 115, 3468–3478. https://doi.org/10.1016/j.rse.2011.08.010.

Whittaker, R.H., 1972. Evolution and measurement of species diversity. Taxon 21, 213–251. https://doi.org/10.2307/1218190.

Zellweger, F., De Frenne, P., Lenoir, J., Rocchini, D., Coomes, D., 2019. Advances in microclimate ecology arising from remote sensing. Trends Ecol. Evol. 34, 327–341. https://doi.org/10.1016/j.tree.2018.12.012.